

# Emergence of spin-active channels at a quantum Hall interface

Amartya Saha,<sup>1</sup> Suman Jyoti De,<sup>2</sup> Sumathi Rao,<sup>2</sup> Yuval Gefen,<sup>3</sup> and Ganpathy Murthy<sup>1</sup>

<sup>1</sup>*Department of Physics and Astronomy, University of Kentucky, Lexington KY 40506-0055, USA*

<sup>2</sup>*Harish-Chandra Research Institute, HBNI, Chhatnag Road, Jhansi, Allahabad 211019, India*

<sup>3</sup>*Department of Condensed Matter Physics, Weizmann Institute, 76100 Rehovot, Israel*

(Dated: March 3, 2022)

We study the ground state of a system with an interface between  $\nu = 4$  and  $\nu = 3$  in the quantum Hall regime. Far from the interface, for a range of interaction strengths, the  $\nu = 3$  region is fully polarized but  $\nu = 4$  region is locally a singlet. Upon varying the strength of the interactions and the width of the interface, the system chooses one of two distinct edge/interface phases. In phase A, stabilized for wide interfaces, spin is a good quantum number, and there are no gapless long-wavelength spin fluctuations. In phase B, stabilized for narrow interfaces, spin symmetry is spontaneously broken at the Hartree-Fock level. Going beyond Hartree-Fock, we argue that phase B is distinguished by the emergence of gapless long-wavelength spin excitations bound to the interface, which can, in principle, be detected by a measurement of the relaxation time  $T_2$  in nuclear magnetic resonance.

*Introduction:* In the integer quantum Hall effect (IQHE), [1] a two-dimensional electron gas (2DEG) subjected to a strong perpendicular magnetic field displays a Hall conductivity quantized in integral units of  $\frac{e^2}{h}$  at low temperatures. These systems are the simplest examples of topological insulators (TIs)[2]. Their bulk is insulating, and the underlying band topology manifests itself in chiral current-carrying edge states which are protected against localization. The topological nature of the bulk state dictates the charge Hall and thermal Hall conductances. In addition, because the kinetic energy is quantized into degenerate Landau levels (LLs), partially filled LLs host the strongest possible electron correlations, leading to quantum Hall ferromagnetism[3, 4] and the fractional quantum Hall effects[5].

Edges play a central role in the QHE, and it has long been realized that within the topological constraints imposed by the bulk, a variety of reconstructed edge phases are possible. Much theoretical work exists on edge reconstructions, with most reconstructions being driven by electrostatic considerations: The “desire” of the electron fluid to perfectly neutralize the positive background competing with the “desire” to form incompressible droplets. In the simplest reconstructions spin plays no role[6–11].

Generically, at the edges of quantum Hall ferromagnets, states with broken spin and/or edge translation symmetry are known to occur in the Hartree-Fock (HF) approximation. [12–15]

It is clear from previous work that edge reconstructions can generate counterpropagating pairs of chiral charge modes. Going beyond previous work, one can ask whether exchange can lead to the emergence of a pair of chiral, neutral, spin-active edge modes. Since spin is involved, at least one of the two bulk quantum Hall states must be a QH ferromagnet.

Motivated by these considerations, we investigate an interface between a  $\nu = 4$  singlet region and a fully polarized  $\nu = 3$  region in the Hartree-Fock (HF) ap-

proximation. In the following, we will use the words edge and interface interchangeably. Our tuning parameters are the width of the interface measured in units of magnetic length ( $\tilde{w} = w/\ell$ ), where the background charge is assumed to vary smoothly between  $\nu = 4$  and  $\nu = 3$ , and the strength of the Coulomb interaction relative to the cyclotron energy ( $\tilde{E}_c = \frac{e^2}{\epsilon\ell\hbar\omega_c}$ ). We find two robust phases: For large  $\tilde{w}$  we find phase A: all HF single-particle levels are spin polarized and three of them cross the Fermi energy, as required by the total  $S_z = 0$  in the  $\nu = 4$  bulk and the total  $S_z = 3/2$  in the  $\nu = 3$ . For smaller  $\tilde{w}$  we find phase B, with spontaneously broken  $U(1)$  spin-rotation symmetry, and a single HF level crossing the Fermi energy appears.

Phase A is conventional, with a pair of counterpropagating, spin-resolved chiral charge modes in addition to the one chiral charge mode required by topology. Phase B, as we will argue in the discussion, manifests a pair of chiral, counterpropagating spin-active neutral modes bound to the interface, in addition to the required charged chiral. Any probe sensitive to gapless long-wavelength spin excitations, such as nuclear magnetic resonance (NMR), will be able to distinguish the two phases.

In the following, we will set up the problem, explain our computation briefly, and describe the two phases in HF. We address the important issue of fluctuations beyond the HF approximation in the discussion, before addressing potential experimental signatures. Details of the robustness of the two phases with respect to the Zeeman coupling ( $\tilde{E}_Z = \frac{E_Z}{\hbar\omega_c}$ ), the screening of the interaction, the number of Landau levels kept in our calculation, and other details, are relegated to the supplemental material (SM) [16].

*Edge between  $\nu = 4$  and  $\nu = 3$  quantum Hall states:* The geometry of the interface between the  $\nu = 4$  and  $\nu = 3$  QH systems is shown in Fig.1. In the non-interacting limit, the  $\nu = 4$  bulk will have the Landau levels (LLs)

$|0 \uparrow, 0 \downarrow, 1 \uparrow, 1 \downarrow\rangle$  occupied, while the  $\nu = 3$  bulk has the LLs  $|0 \uparrow, 0 \downarrow, 1 \uparrow\rangle$  occupied. In this case, at the edge between the two, we expect the  $1 \downarrow$  LL to smoothly cross the chemical potential  $\mu$  from below as one moves rightwards (from  $\nu = 4$  to  $\nu = 3$ ), leading to a single chiral charged edge mode with  $\downarrow$ -spin.

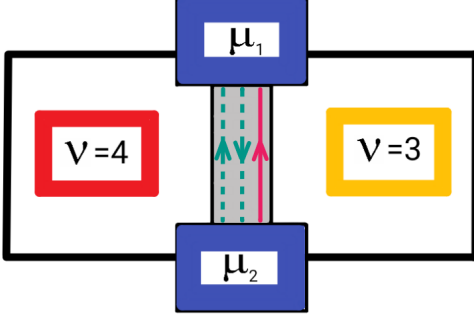


FIG. 1. A schematic diagram of our setup with an interface between bulk  $\nu = 4$  and  $\nu = 3$  IQHE states. The solid line (red online) is a downstream chiral charged mode required by topology. The pair of dashed lines (green online) depict either spin-resolved charged chiral modes (phase A) or gapless spin-active chiral modes (phase B).

As interactions grow stronger we expect a greater tendency towards spin polarization (QH ferromagnetism). However, the  $\nu = 3$  and  $\nu = 4$  states do not get polarized at the same value of  $\tilde{E}_c$ . There is a range of  $\tilde{E}_c$  where the  $\nu = 4$  bulk remains unpolarized, while the  $\nu = 3$  bulk is fully polarized. Now it is no longer obvious how many  $\mu$  crossings, and hence chiral modes, there should be: The result will depend on the details of the interface. Our goal is to study the possible edge phases that can exist as our tuning parameters  $\tilde{w}$ ,  $\tilde{E}_c$  are varied.

The bulk Hamiltonian for a quantum Hall system is

$$H = \hbar\omega_c \sum_{n,k,s} c_{nks}^\dagger c_{nks} + \frac{E_Z}{2} \sum_{n,k} (c_{nk\downarrow}^\dagger c_{nk\downarrow} - c_{nk\uparrow}^\dagger c_{nk\uparrow}) + \frac{1}{2\pi A} \sum_{\mathbf{q}} v(\mathbf{q})(\rho_b(-\mathbf{q}) - \rho_e(-\mathbf{q}))(\rho_b(-\mathbf{q}) - \rho_e(-\mathbf{q})). \quad (1)$$

Using  $n$  for the Landau level index and  $k$  for the guiding center index (defined below), the electron density operator is  $\rho_e(x, y) = \sum_s \Psi_s^\dagger(x, y) \Psi_s(x, y)$ , where the electron field operator is  $\Psi_s(x, y) = \sum_{n,k} \Phi_{nk}(x, y) c_{nks}$ , with  $c_{nks}$  being canonical fermion operators.  $v(\mathbf{q})$  and  $\rho_e(\mathbf{q})$  are the Fourier transforms of the long-ranged screened Coulomb potential  $v(\mathbf{r} - \mathbf{r}')$  and  $\rho_e(x, y)$  respectively. We model the background charge density  $\rho_b$  as changing linearly from  $4\rho_0$  to  $3\rho_0$  ( $\rho_0$  is the density of a single filled Landau level) over a distance  $\tilde{w}$  in the  $\hat{y}$  direction as

shown in Fig.2. Note that the background charge density preserves translation invariance in the  $x$  direction. Thus,  $\tilde{w}$  serves as the tuning parameter which controls the softness of the background potential near the interface. As in real samples, the Zeeman coupling  $\tilde{E}_Z > 0$  (but  $\tilde{E}_Z \ll \tilde{E}_c$  and  $\hbar\omega_c$ ). It follows that the spin symmetry of the Hamiltonian is  $U(1)$ .

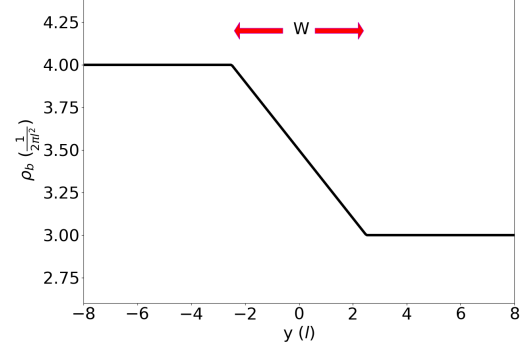


FIG. 2. Dependence of the background charge density on  $\hat{y}$ . The charge density is uniform in the  $\hat{x}$  direction.

For the unscreened Coulomb interaction, at  $\tilde{E}_Z = 0$  in the HF approximation, for  $2.52 < \tilde{E}_c < 2.90$  the bulk  $\nu = 4$  ground state ( $0 \uparrow, 0 \downarrow, 1 \uparrow, 1 \downarrow$  occupied) is unpolarized and the bulk  $\nu = 3$  ground state ( $0 \uparrow, 1 \uparrow, 2 \uparrow$  occupied) is fully polarized. As  $E_z$  increases the range of  $\tilde{E}_c$  changes.

We work in the Landau gauge  $\vec{A} = -B_0 y \hat{x}$  with the magnetic field pointing in the positive  $\hat{z}$ -direction. The magnetic length  $l = \sqrt{\frac{\hbar}{eB_0}}$ . The Hamiltonian has translation invariance along  $x$  (even with the interface potential). The one-body wavefunctions are

$$\Phi_{n,k}(x, y) = \frac{e^{ikx} e^{-\frac{(y-kl^2)^2}{2l^2}}}{\sqrt{L_x n! 2^n \sqrt{\pi} l}} H_n\left(\frac{y-kl^2}{l}\right). \quad (2)$$

The  $x$  coordinate (along the edge) has periodic boundary conditions to discretize  $k$ , which defines the guiding centre position  $Y(k) = kl^2$ . The interface is centred at  $y = 0$  with  $\nu = 4$  as the bulk ground state for  $y < 0$  and  $\nu = 3$  as the bulk ground state for  $y > 0$ . We work in spin-unrestricted HF theory, and look for solutions that preserve the translation invariance in  $x$  of the Hamiltonian, implying that  $k$  is a good single-particle quantum number in HF. Since we allow for Landau level and spin-mixing, we work with a total of 8 basis states for each value of the guiding centre  $k$ , consisting of 4 Landau levels, each with  $\uparrow$  and  $\downarrow$  spins. The translational invariant ground states of the theory are defined in terms of the matrix  $\Delta_{ns,n's'}(k) = \langle c_{n's'k}^\dagger c_{nsk} \rangle$ , which is obtained self-consistently by diagonalizing the effective one-body Hartree-Fock Hamiltonian. The chemical

potential  $\mu$  is chosen to maintain overall charge neutrality. We use a screened Coulomb potential of the form  $v(q) = \frac{2\pi E_c}{q+q_0}$ , where  $q_0$ , the screening parameter, is chosen to be  $q_0 = 0.01$ . Using this method we obtain the phase diagram in the parameters  $\tilde{w}$ ,  $\tilde{E}_c$ .

The SM [16] contains the details of the HF procedure, and an analysis of the stability of our phase diagram with respect to variations in the screening wavevector  $q_0$ , the Zeeman coupling  $E_z$ , and the number of Landau levels that we keep in our calculation.

*Phase diagram in the Hartree-Fock approximation:* There are two distinct edge phases, as shown in Fig.3, separated by a first-order phase transition. In phase A, which is stabilized for very smooth edges, there are three  $\mu$ -crossings of single-particle levels, each spin-resolved. In phase B, stabilized for relatively sharp edges, there is only a single self-consistent energy level that crosses  $\mu$ . In addition, the HF state of phase B shows a spontaneous breaking of the  $U(1)$  spin symmetry.

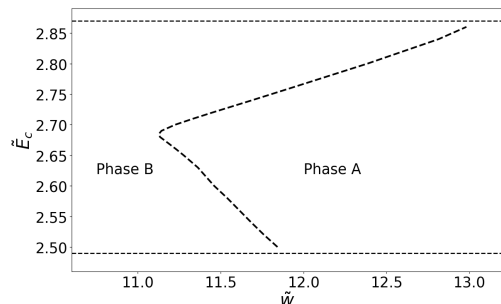


FIG. 3. Phase diagram in the parameter space  $\tilde{E}_c$  and  $\tilde{w}$  at  $\tilde{E}_z = 0.03$ . At this value of  $\tilde{E}_z$  the  $\nu = 4$  bulk state is a singlet and  $\nu = 3$  fully polarized for  $2.49 < \tilde{E}_c < 2.87$ . For values of  $\tilde{E}_c < 2.7$  Landau level mixing is not a significant effect, and the spin-stiffness increases with  $\tilde{E}_c$ . This raises the cost of phase B over phase A, leading to the phase boundary moving towards smaller  $\tilde{w}$ . For  $\tilde{E}_c > 2.7$  Landau level mixing decreases the spin-stiffness, thereby favoring phase B. The transition is first-order in HF.

The main features of the phase diagram result from the competition between (i) the interface potential, controlled by the width  $\tilde{w}$  of the interface region, (ii) the electrostatic repulsion represented by the Hartree term and, (iii) the spin stiffness governed by the Fock term. All three are controlled by the Coulomb interaction. For large values of  $\tilde{w}$ , it is energetically favourable for the system to approximately neutralize the background potential by creating an extra pair of counter-propagating edge modes, spreading the electron density over a larger region. In this phase, the spins of the chiral modes (assuming one associated with each single-particle  $\mu$ -crossing) remain well-defined. For smaller values of  $\tilde{w}$ , it becomes energetically favourable to have a single HF level crossing  $\mu$ . The requirement that the spin polarization at each  $k$

change by  $\frac{3\hbar}{2}$  in going from  $\nu = 4$  to  $\nu = 3$  necessitates a spin rotation (and Landau level index rotation) of all single-particle HF levels, especially occupied ones.

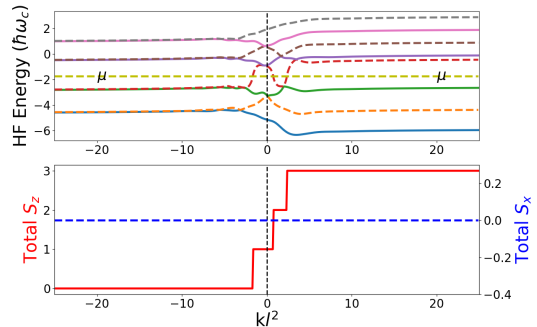


FIG. 4. Phase A in the HF approximation: The upper panel shows the single-particle energy dispersion and the lower panel shows the total  $S_z$  and  $S_x$  values (in units of  $\frac{\hbar}{2}$ ) as a function of the guiding center position. The parameter values are  $\tilde{E}_c = 2.52$ ,  $\tilde{w} = 13.0$  and  $\tilde{E}_z = 0.03$

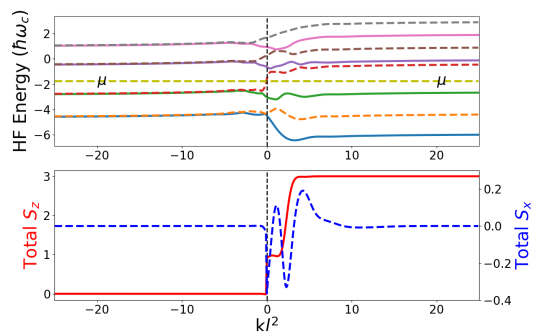


FIG. 5. Phase B in the HF approximation: The upper panel shows the single-particle energy levels and the lower panel shows the total  $S_z$  and  $S_x$  values (in units of  $\frac{\hbar}{2}$ ) as a function of the guiding center position. The parameter values are  $\tilde{E}_c = 2.52$ ,  $\tilde{w} = 10.0$  and  $\tilde{E}_z = 0.03$

Let us examine more closely what we can infer from the HF solution. For this paragraph only, we will make the naive assumption that each single-particle crossing of  $\mu$  represents a chiral mode. The single particle energy levels and the spin components of the levels are plotted in Figs. 4 and 5. From the energy dispersions in Fig.4 we see that two of the modes in phase A are downstream and one is upstream. The spin of these modes can also be explicitly identified as follows. Moving rightwards from large negative  $y$ , first the  $1\downarrow$  level from the  $\nu = 4$  region smoothly crosses  $\mu$  from below, implying a downstream chiral mode with  $\downarrow$  spin. Next the  $2\uparrow$  level crosses  $\mu$  from above, producing an upstream chiral mode with  $\uparrow$  spin. Finally the  $0\downarrow$  level crosses  $\mu$  from below, producing another downstream chiral mode with  $\downarrow$  spin. Note that the spin at the interface changes by three units (each unit is  $\frac{\hbar}{2}$ ) as is required since the bulk state for  $y < 0$  is

the unpolarized  $\nu = 4$  quantum Hall state and the bulk state for  $y > 0$  is the fully polarized  $\nu = 3$  quantum Hall state. Note also that the average value of  $S_x$  remains zero confirming that the chiral levels have well-defined spins. Phase B, on the other hand, has only one chiral downstream mode. Here again, the spin at the interface does change by three units as is required, but the average value of  $S_x$  is non-zero here and there is spin rotation at the interface.

*Discussion of fluctuations beyond HF:* HF is known to broadly overpredict order, due to its neglect of quantum fluctuations. Thus, HF can be taken as reliable for single-particle spectra, but should be supplemented by reasoning based on effective theories when questions of spontaneously broken symmetry and collective modes arise. We will proceed in three steps. (i) We identify the correct effective theory based on symmetries and dimensionality. (ii) We match the HF phases to those of the effective theory by considering a mean-field limit of the effective theory. (iii) We look at quantum fluctuations beyond mean-field in the effective theory, and the implied consequences for physical observables in our system.

The  $SU(2)$  spin symmetry of our electronic Hamiltonian is broken to  $U(1)$  spin rotation around total  $\vec{B}$ , in the presence of Zeeman coupling, and the edge is a quasi-1D system. Thus, the relevant effective theory in the spin sector is the XXZ model in a Zeeman field in 1D[17, 18].  $H_{xxz} = -J \sum S_x(n)S_x(n+1) + S_y(n)S_y(n+1) + \Delta S_z(n)S_z(n+1) - E_z \sum S_z(n)$ .

There is some complicated mapping between our tuning parameters  $\tilde{w}, \tilde{E}_c$  and the XXZ parameters  $J, \Delta$ . To match the phases in HF with those of  $H_{xxz}$ , we take the classical limit of the latter. For  $\Delta < 1$  and  $E_z < 4J(1-\Delta)$ , the XXZ model spontaneously breaks the  $U(1)$  symmetry classically, while for  $\Delta > 1$ , it does not. We conclude that  $\Delta < 1$  in phase B of HF, while  $\Delta > 1$  in phase A.

We finally come to the important issue of quantum fluctuations beyond HF. The Mermin-Wagner theorem[19] ensures that a continuous symmetry cannot be spontaneously broken in 1D, even at zero temperature. Hence the spontaneous breaking of the  $U(1)$  spin-rotation symmetry seen in HF (and the classical limit of  $H_{xxz}$ ) will not survive quantum fluctuations. *However,  $H_{xxz}$  still has two distinct phases.* The distinction between the phases lies in the presence of gapless long-wavelength spin excitations for  $\Delta < 1$ , while they are absent for  $\Delta > 1$ .

The physical consequences for our model system, the  $\nu = 4$  to  $\nu = 3$  interface, are striking. Phase B will have, in addition to the charged chiral edge mode predicted in HF, a pair of gapless, chiral, counterpropagating spin modes bound to the interface. Phase A, on the other hand, simply has three well-separated charged spin-resolved chiral modes (two downstream and one up-

stream). There are no gapless long wavelength spin-flip excitations in phase A.

The classical analysis of  $H_{xxz}$  shows that the system can undergo the  $B \rightarrow A$  transition even for  $\Delta < 1$  upon increasing  $E_z$ . This agrees with the HF analysis (see SM[16]) in which increasing  $E_z$  favors phase A over phase B. It should thus be possible to drive the  $B \rightarrow A$  transition in a given sample by applying an in-plane field.

Let us now examine experimental signatures that distinguish phases A and B. Any probe that couples to low-energy long-wavelength spin fluctuations can be used to tell the phases apart. One such probe is NMR. The nuclear spin moments couple to the external field via their own Zeeman term, and to the electronic spins via the hyperfine interaction. The total electronic spin polarization is measured by the Knight shift [20] of the frequencies of NMR resonance lines. This method has been used to measure the total spin polarization of QH ferromagnets [21–23]. The macroscopic nuclear spin moment relaxes in two ways, firstly via the inhomogeneous distribution of local effective magnetic fields (with relaxation time  $T_1$ ), and secondly via true energy relaxation by emitting and absorbing low-energy electronic spin degrees of freedom (the relaxation time  $T_2$ ). Clearly,  $T_2$  is the relevant quantity to detect the presence or absence of gapless electronic spin excitations. A transition from A to B will lead to a dramatic increase of the energy relaxation rate of nuclear spins, and thus a decrease of  $T_2$ . One complication in our system is that only the nuclear spins near the interface will couple to the gapless chiral spin modes, so a local measurement of  $T_2$  will be necessary. Some progress has been made in this direction recently[24, 25].

We leave several important questions for future analysis. (i) Are there phases besides A and B in a physically realistic model? It seems theoretically possible that in phase B, quantum fluctuations could gap out the spin excitations while leaving the chiral charged edge mode as the sole survivor. Such a phase (call it  $B^*$ ) would be distinct from A because upstream modes (measurable in two-terminal interface charge/thermal conductance) are present in A but absent in  $B^*$ . (ii) What is the order of the  $A \rightarrow B$  transition? The XXZ suggests a  $2^{nd}$  order transition while HF implies  $1^{st}$  order. (iii) Can the gapless chiral spin modes in phase B carry charge? It seems possible that they can, based on the spin-charge relation in QH ferromagnets.

We would like to thank Udit Khanna for many illuminating discussions. We would also like to thank the International Center for Theoretical Sciences, Bangalore, for its hospitality and support during the workshop “Novel Phases of Quantum Matter” (Code: ICTS/Topmatter2019/12). AS and GM would like to thank the US-Israel Binational Science Foundation for its support via grant no. 2016130. SR and GM would like to thank the VAJRA scheme of SERB, India for its support. YG was also supported by CRC 183 (project

C01) of the DFG, the Minerva Foundation, DFG Grant No. RO 2247/8-1, DFG Grant No. MI 658/10-1 and the GIF Grant No. I-1505-303.10/2019. We would also like to thank the University of Kentucky Center for Computational Sciences and Information Technology Services Research Computing for their support and use of the Lipscomb Compute Cluster and associated research computing resources.

- 
- [1] K. v. Klitzing, G. Dorda, and M. Pepper, Phys. Rev. Lett.**45**, 494 (1980).
  - [2] M. Z. Hasan and C. L. Kane, Rev. Mod. Phys.**82**, 3045 (2010).
  - [3] S. L. Sondhi, S. M. Girvin, J. P. Carini, and D. Shahar, Rev. Mod. Phys.**69**, 315 (1997).
  - [4] K. Yang, K. Moon, L. Zheng, A. H. MacDonald, S. M. Girvin, D. Yoshioka, and S.-C. Zhang, Phys. Rev. Lett.**72**, 732 (1994).
  - [5] D. C. Tsui, H. L. Stormer, and A. C. Gossard, Phys. Rev. Lett.**48**, 1559 (1982).
  - [6] D. B. Chklovskii, B. I. Shklovskii, and L. I. Glazman, Phys. Rev. B**46**, 4026 (1992).
  - [7] C. d. C. Chamon and X. G. Wen, Phys. Rev. B**49**, 8227 (1994).
  - [8] J. Dempsey, B. Y. Gelfand, and B. I. Halperin, Phys. Rev. Lett.**70**, 3639 (1993).
  - [9] Y. Meir, Phys. Rev. Lett.**72**, 2624 (1994).
  - [10] J. Wang, Y. Meir, and Y. Gefen, Phys. Rev. Lett.**111**, 246803 (2013).
  - [11] A. H. MacDonald, Phys. Rev. Lett.**64**, 220 (1990).
  - [12] S. L. Sondhi, A. Karlhede, S. A. Kivelson, and E. H. Rezayi, Phys. Rev. B**47**, 16419 (1993).
  - [13] M. Franco and L. Brey, Phys. Rev. B**56**, 10383 (1997).
  - [14] J. H. Oaknin, L. Martin-Moreno, and C. Tejedor, Phys. Rev. B**54**, 16850 (1996).
  - [15] U. Khanna, G. Murthy, S. Rao, and Y. Gefen, Phys. Rev. Lett.**119**, 186804 (2017).
  - [16] Supplemental material.
  - [17] S. Sachdev, *Quantum Phase Transitions* (Cambridge University Press, 2011) 2nd ed.
  - [18] T. Giamarchi and O. U. Press, *Quantum Physics in One Dimension*, International Series of Monographs (Clarendon Press, 2004), ISBN 9780198525004.
  - [19] N. D. Mermin and H. Wagner, Phys. Rev. Lett.**17**, 1133 (1966).
  - [20] C. Slichter, *Principles of Magnetic Resonance*, Springer Series in Solid-State Sciences (Springer Berlin Heidelberg, 1996), ISBN 9783540501572.
  - [21] S. E. Barrett, G. Dabbagh, L. N. Pfeiffer, K. W. West, and R. Tycko, Phys. Rev. Lett.**74**, 5112 (1995).
  - [22] P. Khandelwal, A. E. Dementyev, N. N. Kuzma, S. E. Barrett, L. N. Pfeiffer, and K. W. West, Phys. Rev. Lett.**86**, 5353 (2001).
  - [23] K. R. Wald, L. P. Kouwenhoven, P. L. McEuen, N. C. van der Vaart, and C. T. Foxon, Phys. Rev. Lett.**73**, 1011 (1994).
  - [24] K. F. Yang, M. M. Uddin, K. Nagase, T. D. Mishima, M. B. Santos, Y. Hirayama, Z. N. Yang, and H. W. Liu, New Journal of Physics **21**, 083004 (2019).
  - [25] K. Hashimoto, T. Tomimatsu, K. Sato, and Y. Hirayama, Nature Communications **9**, 2215 (2018).

# Supplemental material for Emergence of spin-active channels at a quantum hall interface

Amartya Saha,<sup>1</sup> Suman Jyoti De,<sup>2</sup> Sumathi Rao,<sup>2</sup> Yuval Gefen,<sup>3</sup> and Ganpathy Murthy<sup>1</sup>

<sup>1</sup>*Department of Physics and Astronomy, University of Kentucky, Lexington KY 40506-0055, USA*

<sup>2</sup>*Harish-Chandra Research Institute, HBNI, Chhatnag Road, Jhansi, Allahabad 211019, India*

<sup>3</sup>*Department of Condensed Matter Physics, Weizmann Institute, 76100 Rehovot, Israel*

In this set of supplemental materials, we provide the details of our theoretical calculations and, importantly, the checks that we have made regarding the robustness of the phases and the phase diagram with respect to various deformations of the theory. In Section I, we establish our notation and briefly recapitulate the Hartree-Fock (HF) method. Next, in Section II we study how the phase diagram changes when we include different numbers of Landau levels in our calculation. Here, we present the phase diagram with three Landau levels and contrast it to the phase diagram with four Landau levels (shown in the main text). In Section III, we study how the phase diagram changes when we change the Zeeman energy and see how phase A expands (in most of the parameter space) at the expense of phase B when we increase the Zeeman energy. We also describe the various checks that we made of the stability of the phase diagram to a change in the screening length, and to changes in the ratio of the Hartree and exchange terms.

## I. THE BASIC SETUP AND NOTATIONS

The notation used here essentially follows the notation given in the supplemental material of an earlier paper[1] co-authored by some of the present authors. As discussed in the main paper, we are studying the ground state of a system with an interface between a  $\nu = 3$  quantum Hall region and a  $\nu = 4$  quantum Hall region. We study the interacting Hamiltonian by using the self-consistent Hartree-Fock approximation. We first decompose the interaction term in the Hamiltonian into Hartree ( $V_H$ ) and Fock ( $V_F$ ) terms by assuming averages of the form

$$\langle c_{n_1 k_1 s_1}^\dagger c_{n_2 k_2 s_2} \rangle = \delta_{k_1, k_2} \Delta_{n_1 s_1; n_2 s_2}(k_1). \quad (\text{S1})$$

We assume that the state has translation invariance along x-direction (along the edge), which leads to the guiding center index  $k$  being a conserved quantity in HF.

In the translation invariant bulk there is no mixing between Landau levels in HF. Further, when the Zeeman term is nonzero, the spin of the single-particle bulk HF states are good quantum numbers, implying that  $\Delta$  becomes diagonal in both Landau level and spin indices and is given by the single-particle occupation  $n_f(n, s)$ . Also, in the bulk, due to charge neutrality, the Hartree potential cancels the background potential and the energy of

the single-particle HF level is

$$E(n_f(m_1, s)) = \sum_{m_2} [\delta_{m_1, m_2} m_1 \hbar \omega_c - E_{ex}(m_1, m_2) n_f(m_2, s)] \quad (\text{S2})$$

where the exchange energy is

$$E_{ex}(m_1, m_2) = \frac{1}{2} \int \frac{d^2 q}{(2\pi)^2} v(\vec{q}) \rho_{m_1 m_2}(\vec{q}) \rho_{m_2 m_1}(-\vec{q}). \quad (\text{S3})$$

The matrix elements of the density operator are, for  $n_1 > n_2$ ,

$$\rho_{n_1 n_2}(\vec{q}) = \sqrt{\frac{n_2!}{n_1!}} \left( \frac{q \ell \exp^{-i\theta_q}}{\sqrt{2}} \right)^{(n_1 - n_2)} L_{n_2}^{(n_1 - n_2)} \left( \frac{q^2 \ell^2}{2} \right) e^{-\frac{q^2 \ell^2}{4}} \quad (\text{S4})$$

where  $L_n^m$  is the associated Laguerre polynomial. For  $n_1 < n_2$  we use  $\rho_{n_2 n_1}(\vec{q}) = (\rho_{n_1 n_2}(-\vec{q}))^*$ . Given the occupations, the bulk ground state energy (at zero Zeeman energy) is

$$\mathcal{E}_{gs} = N_\phi \left( \sum_{m, s} m \hbar \omega_c n_f(m, s) - \frac{1}{2} \sum_{m_1, m_2, s} E_{ex}(m_1, m_2) n_f(m_1, s) n_f(m_2, s) \right) \quad (\text{S5})$$

where  $N_\phi = \frac{e B L_x L_y}{h}$  is the number of flux quanta penetrating the sample.

In our work we use a screened Coulomb interaction, with  $v(q) = 2\pi \hbar \omega_c \tilde{E}_c / (q + q_0)$ , with  $q_0$  being a screening wavevector. The unscreened Coulomb interaction corresponds to  $q_0 = 0$ . Using the expression above one can show that for  $q_0 = 0$ ,  $\tilde{E}_z = 0$ , the bulk  $\nu = 3$  state undergoes a phase transition from a partially polarized state ( $0 \uparrow, 0 \downarrow, 1 \uparrow$ ) to a fully polarized state ( $0 \uparrow, 1 \uparrow, 2 \uparrow$ ) at  $\tilde{E}_c = 2.52$ , whereas for the bulk  $\nu = 4$  state, the phase transition from an unpolarized state ( $0 \uparrow, 0 \downarrow, 1 \uparrow, 1 \downarrow$ ) to a fully polarized state ( $0 \uparrow, 1 \uparrow, 2 \uparrow, 3 \uparrow$ ) occurs at  $\tilde{E}_c = 2.90$ . Hence there exists a regime of  $\tilde{E}_c$  between 2.52 to 2.90, where the  $\nu = 3$  bulk phase is fully polarized and the  $\nu = 4$  bulk phase is unpolarized.

Note that changing the screening length and/or  $\tilde{E}_z = E_z / \hbar \omega_c$  will shift both phase transitions slightly, but

there remains a robust range of  $\tilde{E}_c$  where the  $\nu = 3$  bulk phase is fully polarized and the  $\nu = 4$  bulk phase is unpolarized. The region in parameter space where  $\nu = 4$  is a singlet and  $\nu = 3$  is fully polarized for  $q_0 = 0.01$  is shown in Fig.S1.

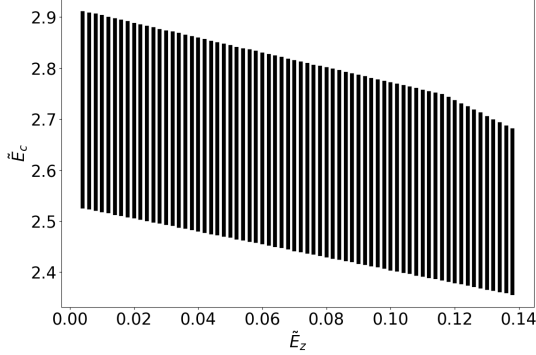


FIG. S1. The shaded region shows where the  $\nu = 4$  bulk is a singlet and the  $\nu = 3$  bulk is fully polarized for  $q_0 = 0.01$ . As  $\tilde{E}_z$  increases, polarized states become lower in energy, and both boundaries shift to lower values of  $\tilde{E}_c$ .

We will be working in the shaded region of the above phase diagram where the structure of the interface between the bulk  $\nu = 4$  and bulk  $\nu = 3$  promises to be interesting - there is a change in spin by  $3/2$  and the occupied Landau levels also change.

Now we go to our system of interest, with an interface between the bulk  $\nu = 4$  and  $\nu = 3$  regions. Once the HF averages are taken, the HF Hamiltonian becomes diagonal in the guiding centre labels  $k$ . The sample is assumed to be an infinite cylinder, with the translation invariant  $x$ -direction taken to be periodic with a finite circumference of  $20\pi l$ , implying that our system has 10 guiding centers per magnetic length  $l$ . We truncate our Hilbert space so that it consists only of 4 Landau levels for each spin. We then define an ‘active’ region with a size of  $50l$  around the origin whose  $\Delta$ -matrix is allowed to vary in the HF procedure, and a ‘frozen’ region on either side of the active region of size  $45l$ , whose occupations are fixed, respectively, to be those of the bulk states  $\nu = 4$  and  $\nu = 3$  to the left and right of the active region. The ‘frozen’ region simulates the Hartree and Fock contributions of the bulk. The self-consistent ground state is then found following a standard iterative procedure, described in detail in Ref.[1]. We have checked that changing the size of the active and frozen regions does not change the results.

## II. THE PHASE DIAGRAM WITH THREE LANDAU LEVELS

In principle, the self-consistent HF should be carried out including Landau level mixing to all Landau levels. This being computationally impossible, one is forced to truncate the Hilbert space by eliminating the Landau levels beyond some cutoff. In the main paper we have quoted our HF results keeping four Landau levels in the calculation. We find two distinct edge phases - phase A obtained for smooth edges or large values of  $\tilde{w} = w/l$  with three spin-resolved chiral modes and phase B obtained for sharp edges with a single chiral mode with spin rotation, and obtained the phase diagram of the two phases in the  $\tilde{E}_c - \tilde{w}$  plane.

In this section, we present the phase diagram when only three Landau levels are kept in the HF calculation (which is the minimum needed to accommodate the fully polarized  $\nu = 3$  state). This allows us to “switch off” some of the Landau-level mixing, and allows us to infer what would occur if we kept even more Landau levels than the four we keep.

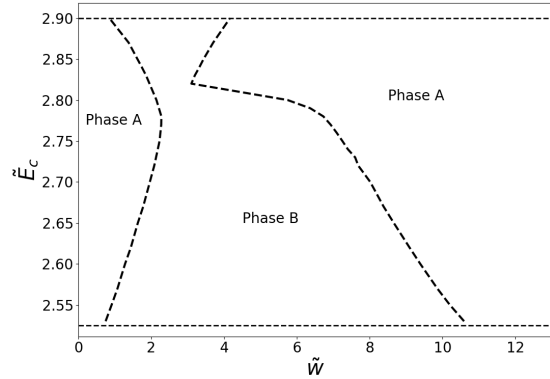


FIG. S2. Phase diagram in the parameter space of  $\tilde{E}_c$  and  $\tilde{w}$  at  $\tilde{E}_z = 0.002$  when only three Landau levels are kept in the HF calculation. The horizontal lines demarcate the upper and lower bounds of  $\tilde{E}_c$  between which bulk  $\nu = 4$  is a singlet and bulk  $\nu = 3$  is fully polarized

As we see in Fig.S2, while the phase diagram for  $\tilde{w} > 3$  is quite similar to that with four Landau levels kept, there is a difference at smaller  $\tilde{w}$ , with phase A being re-entrant at most values of  $\tilde{E}_c$ . However, the difference between the ground state energies of the two phases is extremely tiny in this region of the phase diagram. Increasing Landau level mixing has the primary effect of reducing the spin-stiffness, which lowers the energy of phase B without much altering that of phase A. Hence, it is plausible that including more Landau levels in the calculation will only further favor phase B, and that the phase diagram with four Landau levels kept is qualitatively correct.

We have checked the stability of the phase diagram

with four Landau levels kept by increasing  $\tilde{E}_z$  to 0.2 and we found phase A to be absent for small values of  $\tilde{w}$ . In the following section we will see in more detail the effect of  $\tilde{E}_z$  and  $q_0$  on our phase diagram.

### III. ROBUSTNESS WITH RESPECT TO SCREENING AND THE ZEEMAN COUPLING

In this section, we study the stability of the phase diagram when the various parameters in the theory are changed. Our main aim here is to show that the HF phase diagram presented in the main text is robust to variations of interaction parameters and  $E_z$  within reasonable, physically relevant limits.

#### A : Variation with respect to the Zeeman energy $\tilde{E}_z$

In *GaAs*, in a magnetic field purely perpendicular to the sample, the physical value of the Zeeman coupling is  $\tilde{E}_z \approx 0.03$ . In the main text, all the plots have been shown for  $\tilde{E}_z = 0.03$ .

Here, we restrict ourselves to keeping three Landau levels in the HF calculation, which eases the computational burden enough to allow us to go to low values of  $\tilde{E}_z$  for all  $\tilde{w}$ . We will concentrate on the part of the phase diagram with  $\tilde{w} > 3$ , which as we have seen in the previous section, is qualitatively identical to the phase diagram obtained by keeping four Landau levels. We note that increasing  $\tilde{E}_z$  robustly favors phase A for smaller  $\tilde{E}_c$ , but narrowly favors phase B for larger  $\tilde{E}_c$ .

From the Feynman-Hellman theorem, it is clear that

$$\frac{1}{N_\phi} \frac{\partial \mathcal{E}_{gs}}{\partial E_z} = -\langle HF | S_z^{tot} | HF \rangle \quad (S6)$$

where the average on the right is in the HF ground state. Clearly, the state with the larger average  $S_z$  is favored upon increasing  $E_z$ . In Fig.S4 we can see that for  $\tilde{E}_c < 2.57$ , the total spin polarization of phase B is smaller than that of phase A, and thus phase A expands at the expense of phase B as  $E_z$  increases. The opposite is true for  $\tilde{E}_c > 2.57$ . Since the difference in spin polarizations is smaller for  $\tilde{E}_c > 2.57$ , the shift of the phase boundary is smaller as well. It should be noted that most of the increased spin polarization for larger  $\tilde{E}_c$  occurs in the  $\nu = 4$  region as a result of increased Landau level mixing.

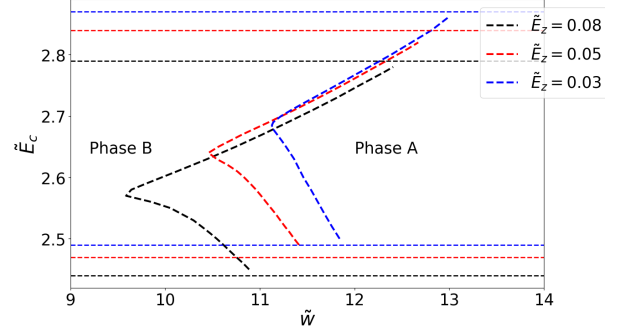


FIG. S3. Phase diagram for different values of  $\tilde{E}_z$ . As earlier, the coloured horizontal lines demarcate the upper and lower bounds of  $\tilde{E}_c$  between which bulk  $\nu = 4$  is a singlet and bulk  $\nu = 3$  is fully polarized for the corresponding values of  $\tilde{E}_z$ .

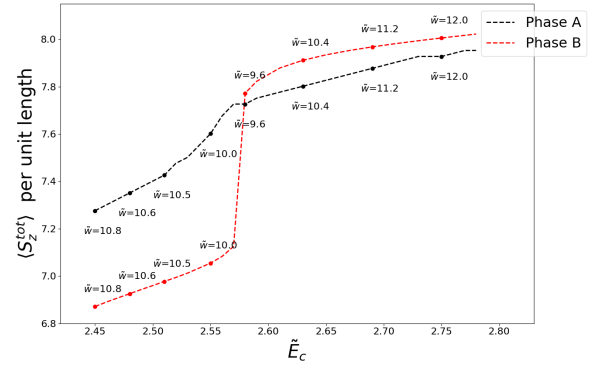


FIG. S4. Magnetization versus  $\tilde{E}_c$  for  $q_0 = 0.01$  and  $\tilde{E}_z = 0.08$ . The  $\tilde{w}$  values at each  $\tilde{E}_c$  are chosen to be at the phase boundary.

#### B: Variation with respect to the screening length

The parameter  $q_0$  is a measure of the inverse screening length. In our main paper we have shown the plots for  $q_0 = 0.01$ . In Fig.S5 we show a comparison of the phase diagram between  $q_0 = 0.01$  and  $q_0 = 0.1$  which has a smaller screening length as compared to  $q_0 = 0.01$ . As can be seen, the phase diagrams are qualitatively similar, with some quantitative shifts. We thus conclude that the phase diagram is robust to changes in the screening length.



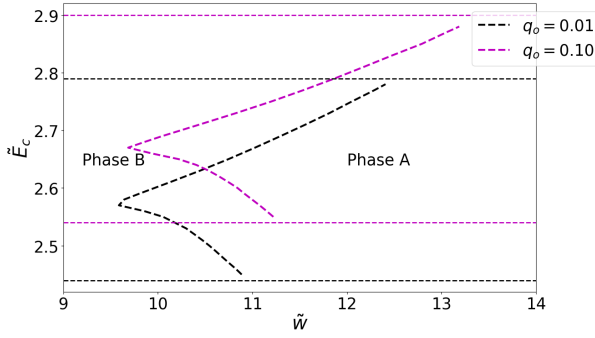


FIG. S5. Phase diagram for different values of the screening length  $q_0$  at  $\tilde{E}_z = 0.08$ . Here again, the coloured horizontal lines demarcate the upper and lower bounds of  $\tilde{E}_c$  between which bulk  $\nu = 4$  is a singlet and bulk  $\nu = 3$  is fully polarized for different  $q_0$  values

### C: Variation with respect to change in ratio of Hartree and exchange terms

We have also varied the ratio of the Hartree and Fock terms to find if Phase A(B) is favored by Hartree or the exchange terms. While this does not correspond to any physical interaction, it can be a useful way to gauge the importance of direct versus exchange terms in the two phases.

We kept the strength of the Fock term at unity, in order to keep the region of  $\tilde{E}_c$  over which the desired bulk states are realized, fixed. The Hartree term was allowed to vary between 0.6 and 1.4. We found that a Hartree term above unit strength favors phase A (the region of phase A expands at the expense of phase B), while a Hartree term below unit strength favors phase B.

- 
- [1] U. Khanna, G. Murthy, S. Rao and Y. Gefen, Phys. Rev. Lett.**119**, 186804 (2017)